Narrow-linewidth interwell THz intersubband emission

Benjamin S. Williams, Bin Xu, Qing Hu, Michael Melloch

Abstract **– Narrow-linewidth terahertz spontaneous emission resulting from interwell (or diagonal) intersubband transition from an electrically pumped multiple quantum-well (MQW) structure was observed. The center frequency of the emission peak is at 2.57 THz, and its full width at half maximum (FWHM) is 0.47 THz. The emission frequency is in good agreement with the calculated intersubband transition energy of 11.3 meV (corresponding to 2.7 THz) in a three-level system, which was designed to achieve population inversion between two radiative levels using LO-phonon assisted depopulation.**

I. Introduction

Spontaneous emission based on intersubband transitions was first observed in the far-infrared or terahertz (THz) frequency range[1]. However, lasers based on intersubband transitions have been developed only in the mid-infrared frequencies. In principle, intersubband lasers could be made to operate at much longer wavelengths by tailoring the design of suitable quantum-well structures. Compared to mid-infrared intersubband lasers, intersubband THz lasers require a more precise control of electron transport as well as new methods for optical mode confinement.

THz intersubband emissions with narrow linewidths (the inverse of which is proportional to the peak gain) have been measured from devices based on intrawell (vertical) intersubband transitions [2],[3],[4]. The scheme of intrawell intersubband transition is known to yield a large radiative dipole moment and a lesser sensitivity to interface roughness. Both features are advantageous to achieve a narrow emission linewidth. However, intrawell schemes also typically possess higher current densities due to faster non-radiative scattering mechanisms. Also, it is difficult to implement a three-level system utilising LO-phonon assisted depopulation based on an intrawell transition scheme. The bottom of the lasing well must be raised relative to the rest of the structure so that the lower radiative level can be emptied by emitting longitudinal optical (LO) phonons, whose energy (36 meV or 9 THz) is at the upper end of the THz spectrum. Raising the bottom of the well would require adding aluminum to the well material GaAs, which would result in a much broader emission linewidth due to alloy scattering [5]. Furthermore, because of the uncertainty in the conduction band offset between $Al_xGa_{1-x}As$ and GaAs and the poor accuracy in controlling the Al mole fraction for small values of x ~ 0.05, an accurate energy alignment between the levels in the lasing well and the rest of the structures will be difficult to achieve. Because of these issues, all previous narrow-linewidth THz intersubband emissions were obtained from two-level systems with miniband injectors, and the population inversion will sensitively depend on the details of electron-electron scattering. In this letter, we report our measurements of narrow-linewidth THz emission that results from interwell (or diagonal) intersubband transitions from a three-level system, whose second level can be emptied by fast LO-phonon scattering.

The MQW structure is based around a core three-level system constructed from a $GaAs/Al_{0.3}Ga_{0.7}As$ triple-quantum-well structure, as shown in Fig. 1(a). The conduction band profile, subband energies, and wavefunctions (magnitude square) were calculated by self-consistently solving the Schrödinger and Poisson equations in the effective mass approximation. The three

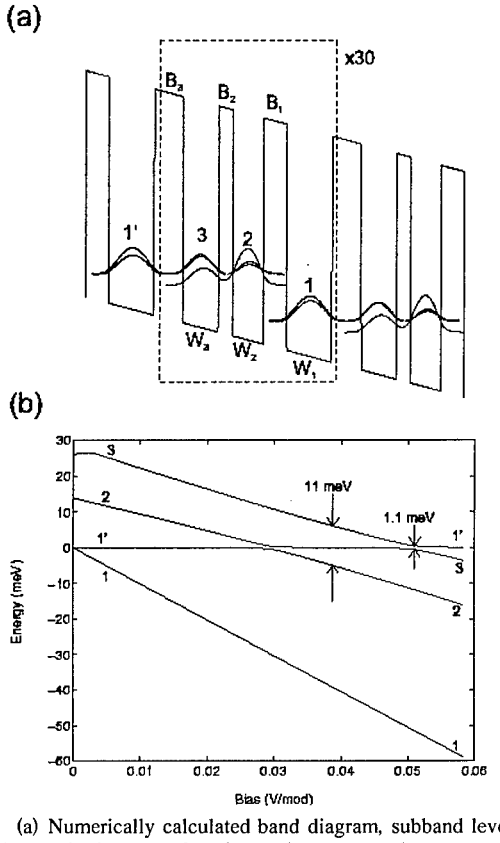

Fig. 1. (a) Numerically calculated band diagram, subband levels, and squared magnitude wave functions of two cascade-connected triple quantum-well modules under a bias of 51 mV/module. (b) Energy levels in the triple-well module vs. bias. E_1' is the injection level from the previous module and is set to zero.

barriers B_1 (4.5 nm), B_2 (2.8 nm), B_3 (5.6 nm), and three wells W_1 (8.8 nm), W_2 (5.9 nm), and W_3 (6.8 nm) form the triple-well module. E_1, and E_2, and E_3 are the ground

B. Williams, B. Xu, and Q. Hu are with the Massachusetts Institute of Technology, Cambridge, Massachusetts 02139.
M. Melloch is with Purdue University, West Lafayette, Indiana 47907.

states in each well, and together they form a three-level system. Thirty such three-well modules were cascaded together and grown by MBE on a n^+ GaAs substrate between n^{++} contact layers.

The designed bias for the THz emission MQW structure is 51 mV per module, at which point the ground state of a previous module E_1' is aligned with E_3, and electrons populate the upper level of the three-level system via resonant tunneling. Electrons make a radiative transition to E_2 and emit a THz photon corresponding to the energy separation E_{32} = 11.3 meV (2.7 THz). At this bias, E_1' and E_3 are anticrossed and their wavefunctions are heavily mixed, which allows us to treat them as a combined doublet state. All the properties related to E_3 were calculated for the combined E_1'/E_3 state. The anticrossing gap between E_1' and E_3, determined by the thickness of B_3, is 1.1 meV, as shown in Fig. 1(b). This anticrossing gap will broaden the THz emission spectra, since electrons will occupy both E_3 and E_1' levels under the resonant tunneling condition.

Non-radiative scattering from levels 2→1 and 3→1 is dominated by LO-phonon scattering. The LO-phonon scattering rates were calculated using the dielectric continuum model to account for the full complex phonon spectra [6],[7], including interface modes and confined modes. The energy separation between E_2 and E_1 (~40 meV) is designed to be slightly greater than the GaAs LO-phonon energy (~36 meV), so that electrons on the E_2 level can be depopulated by "GaAs-like" LO-phonon scattering with a time $\tau_{21} \approx 58$ ps. For non-zero electron temperatures, the scattering time decreases to as low as 40 ps due to activation of "AlAs-like" interface phonon modes (~48 meV). The parasitic scattering time from E_3 to E_1 is $\tau_{31} \approx 95$ ps, which is much longer than τ_{21} because of the reduced wavefunction overlap. These LO-phonon scattering times are longer than the typically picosecond-scale times seen for intrawell transitions due to the use of relatively thick barriers to keep the current density low. The scattering process from E_3 to E_2 is due to a combination of acoustic-phonon scattering, electron-electron scattering, and LO-phonon scattering of hot electrons [8],[9]. Consequently, population inversion could be achieved between E_3 and E_2 levels, if τ_{21} is made smaller than τ_{32}.

The energy separation of the two radiative subbands is designed to be close to their anticrossing gap. As a result, the wavefunctions of the E_3 and E_2 levels have a strong overlap, which yields a large radiative dipole moment (z_{32}=30 Å). This results in a radiative transition lifetime of τ_{rad}=63 μs. Quantum efficiency $\eta \approx \tau_3/\tau_{rad}$ is estimated to be less than 10^{-6}. To assure full carrier ionisation and to eliminate radiative 2p-1s impurity transitions, the Si delta doping was centered in the collector barrier B_1. The actual doping level was measured using capacitive methods [4] to be ~2.5×10^{16} cm^{-3}, or 8.5×10^{10} cm^{-2}/module. This was slightly higher than the designed doping level of 6×10^{10} cm^{-2}/module.

In order to couple out a large portion of the intersubband radiation power from a lossy cavity, we used a diffractive metallic grating with a 15 μm period and a 50% filling factor [10]. This grating, which also served as an ohmic contact, was patterned on top of the device mesas using an annealed Ni/Ge/Au alloy. The measured grating-coupled surface emitter has an area of 415 × 615 μm^2. We also processed smaller unpatterned mesas with a size of 115 × 115 μm^2 to measure the dc current-voltage (*I-V*) relation. Fig. 2 shows the dc *I-V* curve of the MQW structure measured at 4.2 K, along with its differential conductance.

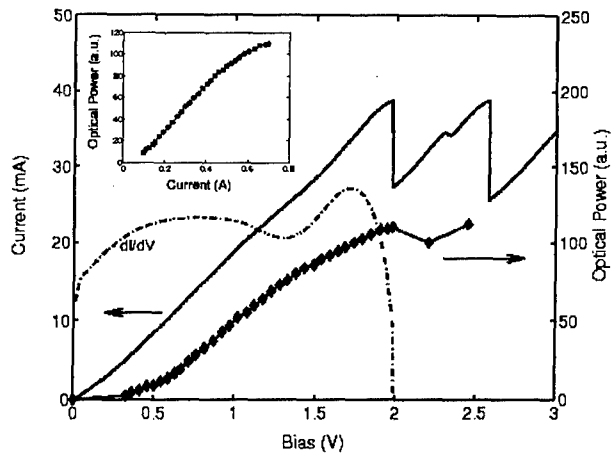

Fig. 2. Measured dc current density and conductance vs. the bias voltage of the 30 module device at 4.2 K. Also plotted is the measured intersubband output power vs. bias and current (inset), which were measured with pulsed bias with the device cooled to 5 K on the cold stage.

The conductance peaks at 1.7 V, indicating the point at which E_1' is aligned with E_3. This is close to the designed bias of 1.53 V (30 × 51 mV), with the extra voltage likely due to the contact resistance. The corresponding current density at this bias is measured to be J_0=254 A/cm^2. At biases greater than 2 V, E_1' becomes misaligned with E_3, resulting in a negative differential resistance. The broader conductance peak centered at 0.7-0.8 V is likely due to the resonant tunneling process of $E_1' \rightarrow E_2$.

For emission measurements, the device was indium soldered to the cold stage in a vacuum cryostat. A free-space Fourier Transform Infrared spectrometer (FTIR) operated in step scan mode was used to resolve emission spectra. A composite silicon bolometer was used in conjunction with a lock-in amplifier to detect the THz radiation. The optical path was purged with nitrogen gas to prevent absorption by water vapor. The bias voltage across the emission device was square-wave modulated at 400 Hz with a 50% duty cycle.

Our optical spectra reveal a clear peak due to the $E_3 \rightarrow E_2$ intersubband emission. A representative spectrum taken at 5 K is shown in Fig. 3(a), which was taken at a bias of 1.6 V (close to the designed value of 1.53 V). The measured peak frequency of 2.57 THz (corresponding to 10.6 meV) is close to the designed value of 11.3 meV. Since $\Delta E = E_3 - E_2$ is designed to be close to the anticrossing gap, E_3 and E_2 track each other as the bias voltage is changed, as shown in Fig. 1(b), and we should expect to see little Stark shift of the emission frequency.

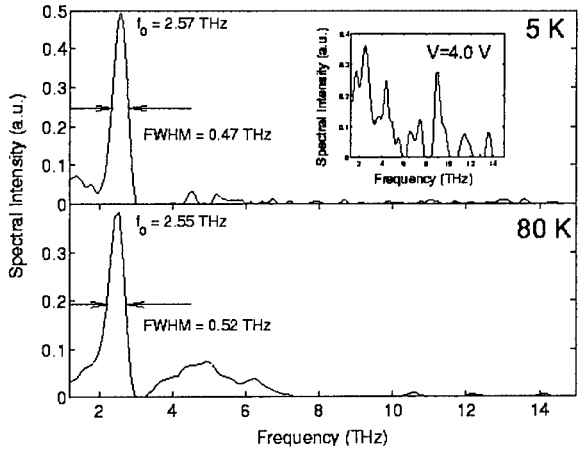

Fig. 3. Spectrally resolved THz intersubband emission taken at (a) 5 K and (b) 80 K under a bias of 1.6 V. The inset shows the spectrum under a 4.0 V bias.

This is indeed the case. In the bias range of 1.0-1.9 V, in which the level E_3 has an appreciable population, the emission spectra showed a narrow peak whose frequency barely changed with the bias voltage. The full-width half-maximum (FWHM) of the emission peak is as narrow as 0.47 THz (1.93 meV). In comparison, the anticrossing gap of E_1' and E_3 is 1.1 meV. At anticrossing, the two levels are spatially extended (as shown in Fig. 1(a)) and both contribute to the intersubband emission signals. Thus, a large fraction of the measured 1.93 meV linewidth is due to the energy splitting of the injection level E_1' and the upper radiative level E_3. Even with 30 modules and a relatively high doping density, the total linewidth broadening due to nonuniformity, interface roughness, impurity and phonon scattering, is only ~0.8 meV. The spontaneous emission linewidth can be further reduced by increasing the thickness of the injection barrier B_3 that will decrease the anticrossing gap between E_1' and E_3, provided that the injection efficiency is still limited by the lifetime τ_3 of the E_3 level [11].

In order to verify the intersubband origin of the measured emission spectra, we have measured emission spectrum at a high bias of 4.0 V at which the energy levels are severely misaligned. The spectrum is shown in the inset of Fig. 3(a), and it bears little resemblance to the main figure.

The emitted intersubband optical power is plotted versus applied bias in Fig. 2, and shows the expected behaviour. Since this power is proportional to the E_3 population, the observed power drops above 2.0 V as the subbands become misaligned. Examination of the power versus current characteristic reveals a slightly sublinear behaviour at higher currents, indicating a decrease in τ_{32} at high populations (due to *e-e* scattering) or currents/temperatures (due to thermally assisted LO-phonon scattering). Interpretation of the *L-I* behaviour cannot be directly compared with that from a two-level system, since at low bias, current flows through level E_2 which emits THz photons at different frequencies. The peak intersubband output power was measured to be several pW, compared with a calculated emission power of approximately 5-10 nW. The large discrepancy is attributed to a combination of low optical collection efficiency, and free carrier losses in the upper layer.

Spectra were also taken with the cold stage cooled with liquid nitrogen to 80 K. At this elevated temperature, the *I-V* characteristics remained principally unchanged, but the emitted optical power due to intersubband transitions was approximately a factor of 2.5 smaller. This difference is due to a reduced scattering time τ_{32} at the elevated temperature. A measured spectrum is shown in Fig. 3(b). The main peak is essentially the same as the one measured at 5 K, with a slightly broader linewidth of 0.52 THz (2.14 meV). The secondary broad feature is blackbody radiation due to device heating. The linewidth measured at 80 K is expected to be similar to that at 5 K, since nonparabolicity is negligible for THz intersubband emitters. Nevertheless, our experimental verification is encouraging for the development of intersubband THz sources at elevated temperatures.

In steady state, the relative population $n_3/n_2 = \tau_{32}/\tau_{21}$, and is a critical parameter in achieving gain. τ_{21} is due to LO-phonon scattering and can be calculated (~40-58 ps). τ_{32}, however, is mainly due to electron-electron scattering and LO-phonon scattering of hot electrons. Both processes depend on the injection levels and it is difficult to accurately calculate the scattering time. Using a rate equation analysis, at design bias the current density is given by $J_0 = eN_D(\tau_{32} + \tau_{31})/((\tau_{32} + \tau_{21})\tau_{31})$. For the calculated values of τ_{21} and τ_{31} however, J_0 (254 A/cm^2) only weakly depends on τ_{32}, and thus an accurate extraction of τ_{32} from experimental data is difficult. Due to the extremely thick collector barrier, and the resulting long τ_{21}, the existence of a population inversion in this particular structure is unlikely. However, in principle, our three-level systems can be easily modified to yield a greater scattering time ratio τ_{32}/τ_{21} by reducing the thickness of the collector barrier B_1. Since this decreases the carrier transit time through a module, the doping density must be reduced to prevent an increase in current density, and a corresponding reduction in τ_{32} due to increased thermally activated LO-phonon scattering.

In summary, we have observed narrow-linewidth intersubband THz emission based on interwell (or diagonal) transitions. This intersubband-transition scheme allows a straightforward implementation of three-level systems, which can be carefully engineered to achieve population inversion at THz frequencies.

This work was supported by AFOSR, NASA, NSF, and ARO.

References

[1] M. Helm, P. England, E. Colas, F. DeRosa, and S. J. Allen, Jr., "Intersubband emission from semiconductor superlattices excited by sequential resonant tunneling," Phys. Rev. Lett. vol. 63, pp. 74-7, 1989.

[2] M. Rochat, J. Faist, M. Beck, U. Oesterle, and M. Ilegems, "Far-Infrared (λ=88μm) electroluminescence in

a quantum cascade structure," Appl. Phys. Lett., vol 73, pp. 3724-6, 1998.
[3] J. Ulrich, R. Zobl, K. Unterrainer, G. Strasser, E. Gornik, "Magnetic field enhanced quantum cascade emission," Appl. Phys. Lett., vol 76, pp. 19-21, 2000.
[4] S. Blaser, M. Rochat, M. Beck, J. Faist, and U. Oesterle, "Far-infrared emission and Stark-cycletron resonances in a quantum cascade structure based on photon-assisted tunneling transition," Phys. Rev. B, vol. 61, pp. 8369-74, 2000.
[5] K. L. Campman, H. Schmidt, A. Imamoglu, and A. C. Gossard, "Interface roughness and alloy-disorder scattering contributions to intersubband transition linewidths," Appl. Phys. Lett., vol. 69, pp. 2554-6, 1996.
[6] H. B. Teng, J. P. Sun, G. I. Haddad, M. A. Stroscio, S. Yu and K. W. Kim, "Phonon assisted intersubband transitions in step quantum well structures," J. Appl. Phys., vol. 84, pp. 2155-2164, 1998.
[7] S. Yu, K. W. Kim, M. A. Stroscio, G. J. Iafrate, J. P. Sun, and G. I. Haddad, "Transfer matrix method for interface optical-phonon modes in multiple-interface heterostructure systems," J. Appl. Phys., vol 82, pp. 3363-3367, 1997.
[8] J. H. Smet, C. G. Fonstad, and Q. Hu, "Intrawell and interwell intersubband transitions in multiple quantum wells for far-infrared sources," J. Appl. Phys., vol 79, pp 9305-20, 1996.
[9] B. Xu, Ph.D. thesis, MIT (1998), unpublished.
[10] B. Xu and Q. Hu, Appl Phys. Lett., "Grating coupling for intersubband emission," vol. 70, pp. 2511-3, 1997.
[11] C. Sirtori, F. Capasso, J. Faist, A. L. Hutchinson, S. L. Sivco, and A. Y. Cho, "Resonant tunneling in quantum cascade lasers," IEEE J. Quantum Electron., vol. QE-34, pp. 1722-9, 1998.